Journal of Environmental Radioactivity 274 (2024) 107409

Contents lists available at ScienceDirect

Journal of Environmental Radioactivity

journal homepage: www.elsevier.com/locate/jenvrad

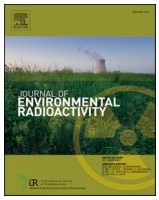

The causes of the abrupt enhancement of the natural gamma radiation in the thunderous atmosphere on the mountain tops

A. Chilingarian *, B. Sargsyan

A I Alikhanyan National Laboratory (Yerevan Physics Institute), Yerevan, 0036, Armenia

ARTICLE INFO

Keywords:
NGR
TGE
Aerosols

ABSTRACT

The study presented the relationship between sudden Natural Gamma Radiation (NGR) increases related to enhanced atmospheric electric fields. We pinpoint Thunderstorm Ground Enhancements (TGEs) as the primary source of abrupt and significant NGR spikes. These TGEs, which are transient, several-minute-long increases in elementary particle fluxes, originate from natural electron accelerators within thunderclouds. The more prolonged, yet less pronounced, increases in NGR, persisting for several hours, are attributed to the gamma radiation from radon progeny and enhanced positron fluxes. This radon, emanating from terrestrial materials, is carried aloft by the Near-Surface Electric Field (NSEF). To measure NGR at Aragats Mountain, we use an ORTEC detector and custom-built large NaI (Tl) spectrometers, employing lead filters to discriminate between cosmic ray fluxes and radon progeny radiation. Our analysis differentiates between radiation enhancements during positive and negative NSEF episodes. The resultant data provide a comprehensive measurement of the intensities of principal isotopes and positron flux during thunderstorms compared to fair weather conditions.

1. Introduction

Natural gamma radiation (NGR) originates from radioactive isotopes in the Earth's crust and Cosmic Rays (CR) interactions in the terrestrial atmosphere. Monitoring NGR levels is crucial for controlling radiation exposure near nuclear power plants, thus ensuring public safety. NGR is the primary source of irradiation that affects the human body (UNSCEAR, 1993), and it is significantly influenced by the geology and geography of a specific region in the world (UNSCEAR, 2000). Therefore, information about NGR is essential for establishing safety standards and national guidelines that align with international recommendations (Abba et al., 2017).

The newly established field of High Energy Physics in Atmosphere (HEPA) researches the effects of cosmic ray flux modulation in the Earth's atmosphere. This includes thunderstorm ground enhancements (TGEs, Chilingarian et al., 2010, 2011), i.e., impulsive enhancement of the cosmic ray fluxes during thunderstorms. These studies shed light on the complex interrelations of the atmosphere and cosmic ray fluxes and the impact of cosmic rays on our planet. Usually, the largest TGEs last a few minutes. During this time, particle fluxes can increase to tens or even hundreds of times the fair-weather values. Lightning flashes abruptly terminate them. During TGEs, lightning activity is usually suppressed. The origin of TGE is the relativistic runaway electron avalanche (RREA, Gurevich et al., 1992; Babich et al., 2001; Alexeenko et al., 2002; Dwyer, 2003) developed in the thunderous atmosphere.

During a 24/7 TGE monitoring campaign with SEVAN detectors (Chilingarian et al., 2022b) at the highest mountains across Eastern Europe, Germany, and Armenia, it has been found that the RREA mechanism is universal and operates in thunderous atmospheres globally. During thunderstorms, there are two additional radiation sources aside from the rather stable radiation from radioactive isotopes and ambient cosmic radiation.

Natural gamma radiation (NGR) primarily emanates from Earth's crust through radioactive decay and interactions between cosmic rays and the atmosphere. Monitoring NGR is vital, especially around nuclear power facilities, to manage radiation levels and safeguard public health. As the leading source of non-medical radiation exposure to humans (UNSCEAR, 1993), NGR varies significantly with local geology and geography (UNSCEAR, 2000). Knowledge of NGR informs the development of safety standards and national regulations, ensuring they align with international benchmarks (Abba et al., 2017).

The emerging High Energy Physics in Atmosphere (HEPA) discipline explores how cosmic ray fluxes are modulated within our planet's atmospheric conditions, including thunderstorm ground enhancements

* Corresponding author.
E-mail address: chili@aragats.am (A. Chilingarian).

https://doi.org/10.1016/j.jenvrad.2024.107409
Received 27 October 2023; Received in revised form 17 February 2024; Accepted 18 February 2024

(TGEs). These phenomena, marked by transient spikes in cosmic ray intensity during thunderstorms, illuminate the intricate dynamics between atmospheric processes and cosmic radiation. Typically, TGEs are short-lived, with the most intense episodes lasting mere minutes but showing particle flux increases that can exceed normal levels by orders of magnitude, often ceasing abruptly with a lightning flash. However, lightning tends to be less frequent during these events. Recently, significant strides have been made in cataloging TGE occurrences, with 650 events documented on Mount Aragats (Chilingarian et al., 2022b) and 80 air glows observed off Japan's western coast (Wada et al., 2021). The consensus attributes TGEs to the relativistic runaway electron avalanche (RREA) mechanism, a process active in electrically charged atmospheres (Gurevich et al., 1992; Babich et al., 2001; Alexeenko et al., 2002; Dwyer, 2003). Continual monitoring with SEVAN detectors has revealed that the RREA mechanism is a global phenomenon in thunderstorms worldwide. Thunderstorms introduce two supplementary sources of the enhanced radiation—the gamma emissions from radon progeny and the increased flux of cosmic rays.

Impulsive radiation from and prolonged radiation from radon progeny lifted by the near-surface electric field (NSEF)—constitute two significant sources of environmental radiation. Fig. 1 illustrates the comprehensive radiation environment, including the detection instruments deployed on Earth's surface and in space. On the diagram's right side, gamma rays and protons, produced by cosmic accelerators like supernova remnants (SNRs), trigger cascades of secondary particles in the Earth's atmosphere. SNRs accelerate protons and nuclei as heavy as iron, while neutron star mergers create the universe's heaviest elements. Upon interacting with Earth's atmosphere, energetic hadrons, leptons, and gamma rays can generate extensive air showers (EASs Auger et al., 1939), producing vast numbers of secondary particles. These EASs are a potent and constant source of free electrons, propelled and multiplied within the strong atmospheric electric fields. At the base of Fig. 1, the Aragats research station—situated at an elevation of 3200 m—is shown, equipped with an array of particle detectors and spectrometers that provide around-the-clock monitoring of virtually all cosmic ray species (Chilingarian et al., 2005).

The lower dipole comprises the same main negative layer in the middle of the thundercloud, and its mirror in the Earth accelerates electrons in the direction of the Earth's surface, sustaining a minute-stable flux of relativistic electrons and gamma rays. All sources of NGR shown in the illustration are merged into a single radiation environment. It's difficult to distinguish the TGE flux from other sources, such as CR secondary flux and radon isotope gamma radiation. As a result, precise measurements of NGR and complex statistical analysis are required to differentiate these sources. When radon gas is released from the basalts of Aragats into the near-surface environment, it is influenced by the NSEF. The decay products of radon-222, commonly known as radon progeny, become electrically charged soon after formation, typically by binding to charged aerosols. When exposed to an electric field, these charged aerosols, with radon progeny attached, are elevated into the atmosphere. This process increases NGR, known as the radon circulation effect Chilingarian et al. (2020). This led to additional gamma radiation contributing to the low energy flux of the TGE. This flux continues even after the electric field strength returns to the fair-weather

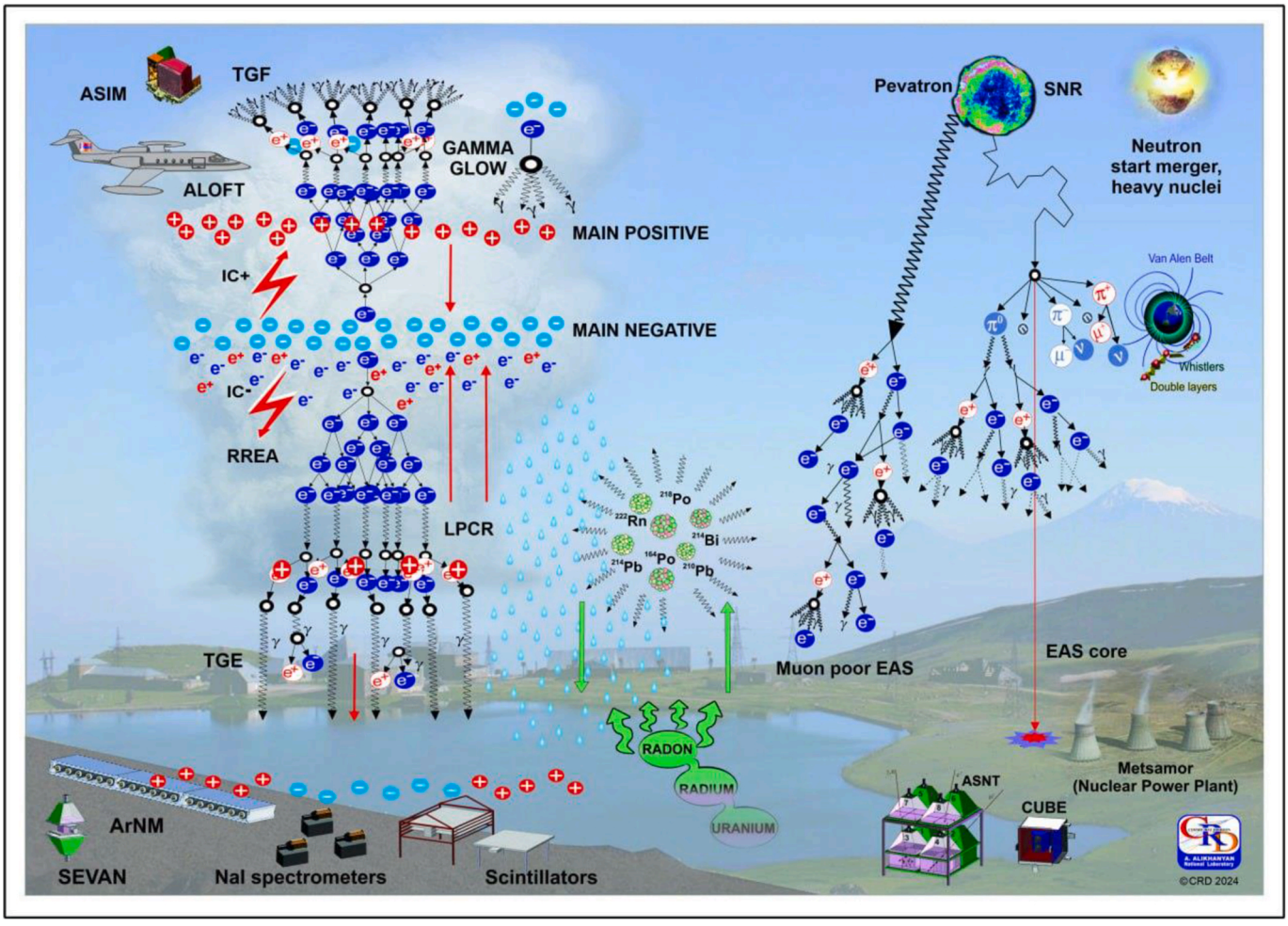

Fig. 1. Various sources of NGR, including fluxes of secondary particles from space and atmospheric accelerators, gamma radiation from ^{222}Rn progeny from Earth's crust, and from the atmosphere.

value due to the tens of minutes-long lifetime of non-stable isotopes ^{214}Pb and ^{214}Bi. Thus, nonstable nuclides comprise a significant portion of the low-energy gamma-ray flux measured by particle detectors and spectrometers at Aragats (Chilingarian et al., 2019).

Fairweather NGR is a mixture of the gamma-ray produced by galactic (and, sometimes, also solar) cosmic rays in interactions with the atmosphere and gamma radiation of several nonstable isotopes emanating from nearby basalts. It is tough to see any "isotope-produced "structures in the resulting spectra of TGE with low-resolution large-size spectrometers used for the monitoring of high-energy (up to 50 MeV) gamma radiation on Aragats (see details of the NaI spectrometers network on Aragats in (Chilingarian et al., 2022a). Numerous TGEs observed on Aragats are an ideal target to investigate the source of the ionization radiation because the low altitude of thunderclouds enables us to detect electrons, gamma rays, and neutrons simultaneously. The joint monitoring of almost all species of cosmic rays, measuring energy spectra of electrons and gamma rays with numerous detectors and spectrometers, is now paired with precise spectroscopy of NGR. By measuring the differential energy spectra of electrons and gamma rays in the energy range from 300 keV to 50 MeV, we discovered that the particle fluxes continued for ~1.5–2 h with a characteristic decay time of ~40–50 min, well coincides with the joint half-life time of isotopes ^{214}Pb (352 keV) and ^{214}Bi (~609 keV) of the uranium-radium chain. We must emphasize that a direct equivalence between the precisely established half-life of specific isotopes and the results of our empirical measurements may not exist. External variables, including aerosol size distribution, the composition of radon progeny, prevailing wind patterns, and the emanation rate of radon gas, affect the rate at which observed radiation intensity decreases. However, while potentially modifying the observed relationship, these factors do not substantially impact the measured half-life in our experiment.

Our paper offers insights into the boost of the NGR during thunderstorms through joint observations of TGEs and NGR with ORTEC and large NaI spectrometers. We aim to understand better the modulation of secondary CR fluxes by strong atmospheric electric fields and analyze the modulation of the energy spectrum of NGR by strong atmospheric electric fields. To address these goals, we have monitored NGR at an elevation of 3200m on Aragats mountain and select periods of the enhanced NSEF separately at positive and negative electric fields. The energy spectra of the main isotopes contributing to NGR are analyzed, and statistical analysis shows significant modulation differences by electric fields of different polarities.

2. Instrumentation

Various particle detectors and spectrometers at Aragats Space Environmental Center (ASEC, Chilingarian et al., 2005) monitor 24/7 particle fluxes of almost all species of the secondary CR flux. We use the ORTEC-905-4 spectrometer for NGR spectroscopy. This gamma spectrometer is equipped with a 3" × 3" NaI (Tl) crystal, has 1024 measuring channels, excellent stability, Fig. 2b. The relative energy resolution of FWHM (full width at half maximum) is approximately 8% at energy levels of 0.3–3 MeV (Hossain et al., 2012). Also, we utilize a network of six large NaI spectrometers to observe TGE gamma radiation, Fig. 2a. The sensitive area of each spectrometer is roughly 0.035m2 (11.5 × 30 cm) with a thickness of 11.5 cm, which is about six times larger than the ORTEC spectrometer's (a cylinder with a 3" length and diameter, cross-section of 0.0056 m^2). The time resolution of spectrometers is ≈ 50μs. These NaI spectrometers provide ample statistics, with 50,000 to 60,000 counts per minute, to recover the TGE energy spectrum in the energy range of 0.3–50 MeV. However, the energy resolution of large NaI spectrometers is much worse than ORTEC's, and we cannot resolve the isotope spectral lines with it. Poor energy resolution turns discrete isotope energies into broad distributions. Combining ORTEC with large NaI spectrometers allows us to perform accurate isotope spectroscopy within the energy range of 0.3–3 MeV. Additionally, we can retrieve energy spectra of up to 50 MeV for the most significant observed TGEs. For more details on the spectrometer and energy recovery method, please refer to (Chilingarian et al., 2022a).

To compare ORTEC and NaI detector's operation in the energy range −0.3–3 MeV, we cover NaI detector N 4 with 4 cm of lead above (Fig. 2a). The high-energy portion of TGE comes mainly from the near-vertical direction (azimuth angles within 0–25°). Thus, the cosmic ray radiation is suppressed, and the spectrometer counts mostly low-energy gamma radiation of the radon progeny coming under large zenith angles. To compare the TGE flux measured by NAI and ORTEC, visa-verse we cover the ORTEC spectrometer, by 4-cm thick lead filter (Fig. 2b) to suppress Radon progeny gamma radiation and outline the enhanced cosmic ray radiation of TGE.

3. Measuring the half-life of radon isotopes with NaI and ORTEC spectrometers

During thunderstorms, the emerged NSEF lifts radon and its progenies to the atmosphere, adding additional gamma radiation to the TGE flux. As the storm finishes, the electric field strength returns to fair-weather value, and the uplift of Rn progenies stops. In Fig. 3, we show the time series of count rates measured by NaI spectrometers N 2 (black curve) and N 4 (blue curve, 4 cm lead on the top) and ORTEC detector count rate (red curve). To scale time series in one picture, we show time series not in absolute counts but relative numbers (percent to fair weather value). By the green lines, we outline the period when we compare the mean count rates of three detectors (Table 1). In the time series of the NaI N2, we can see prominent peaks from the TGE particles

Fig. 2. Large NAI spectrometer with lead filters above a); ORTEC spectrometers with lead filters from the sides and the bottom b).

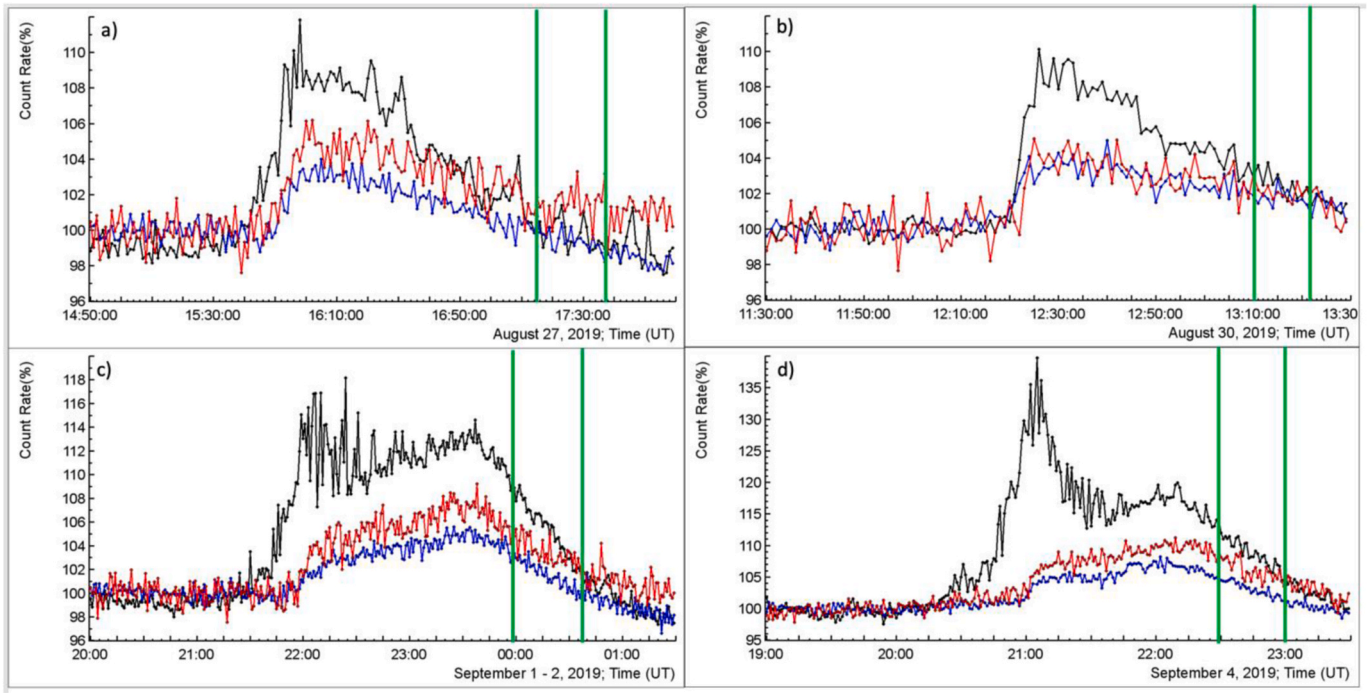

Fig. 3. One-minute time series of count rates of NaI spectrometers N2 (black, energy threshold 0.3 MeV), N4 (blue, energy threshold 0.3 MeV, 4 cm lead filter on the top), and ORTEC spectrometer (red). Green lines show the time when the mean count rates in Table 1 were calculated. Frames (a–d) correspond to the first four rows of Table 1. (For interpretation of the references to colour in this figure legend, the reader is referred to the Web version of this article.)

Table 1
Mean count rates of 3 detectors measured after the storm at fair weather in the decay phase of TGE (radon progeny gamma radiation only).

2019	NaI N4 cnts/ min	NaI N2 cnts/ min	ORTEC cnts/ min	NaI N4/ ORT	NaI N2/ ORT	NaI $T_{0.5}$ (min)	ORTEC $T_{0.5}$ (min)
27/ 08	40,841 ± 318	57,728 ± 938	13,435 ± 130	3.04	4.30	52	51
30/ 08	41,030 ± 282	56,882 ± 571	13,286 ± 114	3.08	4.28	46	47
2/09	40,800 ± 382	57,774 ± 982	13,755 ± 153	2.97	4.16	50	50
4/09	43,080 ± 402	63,024 ± 403	14,380 ± 154	3.00	4.38	49	46
6/09	41,771 ± 296	58,763 ± 716	13,663 ± 160	3.06	4.30	48	49
11/ 09	39,825 ± 191	52,746 ± 371	13,282 ± 134	3.00	3.97	40	40
17/ 09	39,724 ± 271	55,492 ± 511	13,185 ± 112	3.0	4.21	50	48
28/ 09	38,743 ± 440	54,061 ± 690	13,567 ± 165	2.86	4.01	51	50
Mean	40,727 ± 230	57,059 ± 340	13,569 ± 140	3.00 ± 0.06	4.2 ± 0.13	46 ± 4,5	47 ± 3,3

coming from the near-vertical direction. In the count rates of NaI 4, TGE particles are suppressed due to the 4 cm lead filter above. The count rates we measure are susceptible to fluctuations due to changes in atmospheric pressure, influencing the cosmic ray flux and temperature drift, which can affect the performance of the NaI scintillator. We continuously monitor atmospheric pressure and temperature with a DAVIS weather station to address this and select TGE events with stable environmental parameters. Atmospheric factors typically manifest their effects over longer durations than our observed flux enhancements. Episodes of count rate increases have been carefully selected for analysis when peak enhancements exceed 10%, corresponding to a statistical significance of over 7σ.

Table 1 shows the mean count rates (cnts) of 8 TGEs that occurred during one month in August–September 2019, measured by three spectrometers. The 1-min count rates were averaged over time of the decay phase of TGE at fair weather when there were no disturbances of NSEF and TGE flux. The ratio of count rates of NaI N4 (second column) to ORTEC (fourth column) is very stable at 3.00 ± 0.06, confirming that both spectrometers are measuring the same radon progeny gamma radiation coming under large zenith angles. The ratio of counts NaI N2 to ORTEC is more vulnerate at 4.2 ± 0.13, reflecting fluctuation of the near-vertical flux registered by the NaI N2. The last two columns show the recovered half-life time of the radon progeny gamma radiation estimated by NaI (Tl) and ORTEC spectrometers.

In Fig. 4, we demonstrate the data used to recover the half-life time measured by two spectrometers, which fit each other precisely. The half-life of count rate decay (40–50 min for all considered TGEs) corresponds to the joint half-life of the most-abundant gamma emitters from the Rn chain, namely, ^{214}Pb (the half-live time ≈27 min) and ^{214}Bi (the half-live time ≈20 min). Note that the "offset" term of fit in the legend of Fig. 4 represents the vertical shift and corresponds to the count rates of NaI N4 and ORTEC spectrometers. Their ratio again is 3 with high precision.

Thus, measurements of NGR made by the ORTEC and NaI spectrometers are equivalent and can be used to disentangle cosmic ray flux and isotope gamma radiation.

4. Recovery of NGR from the ORTEC and NaI spectrometric measurements

Fig. 5a shows the NGR spectrogram measured by the ORTEC spectrometer. We can see a significant contribution of the CR flux, making a "pedestal" in the spectrogram. To convolute the NGR and CR, we use measurements of NaI spectrometers with and without lead filter above. We cannot use NaI measurements for NGR estimation because the resolution of the spectrometer is poor, 50–60% at energies below 3 MeV, and isotope peaks are smeared. However, spectrometers are sensitive to energies up to 100 MeV with better resolution, which is crucial for proving the RREA-TGE mechanism. We obtain the CR contribution to

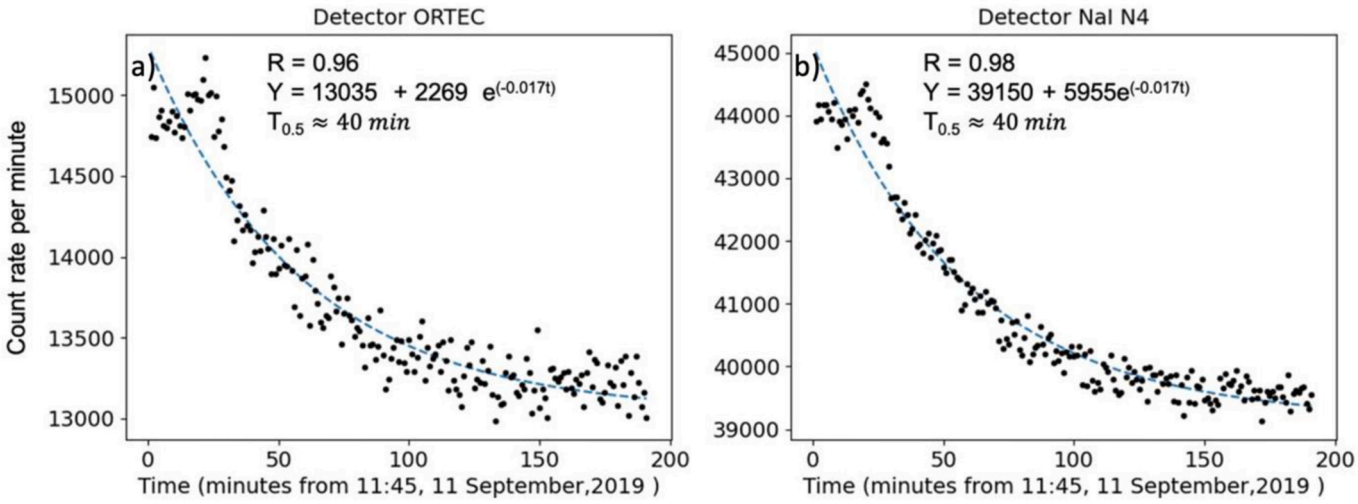

Fig. 4. Calculation of the half-life time ($T_{0.5}$) of the radon progenies lifted to the atmosphere by the NSEF disturbed during thunderstorms on Aragats.

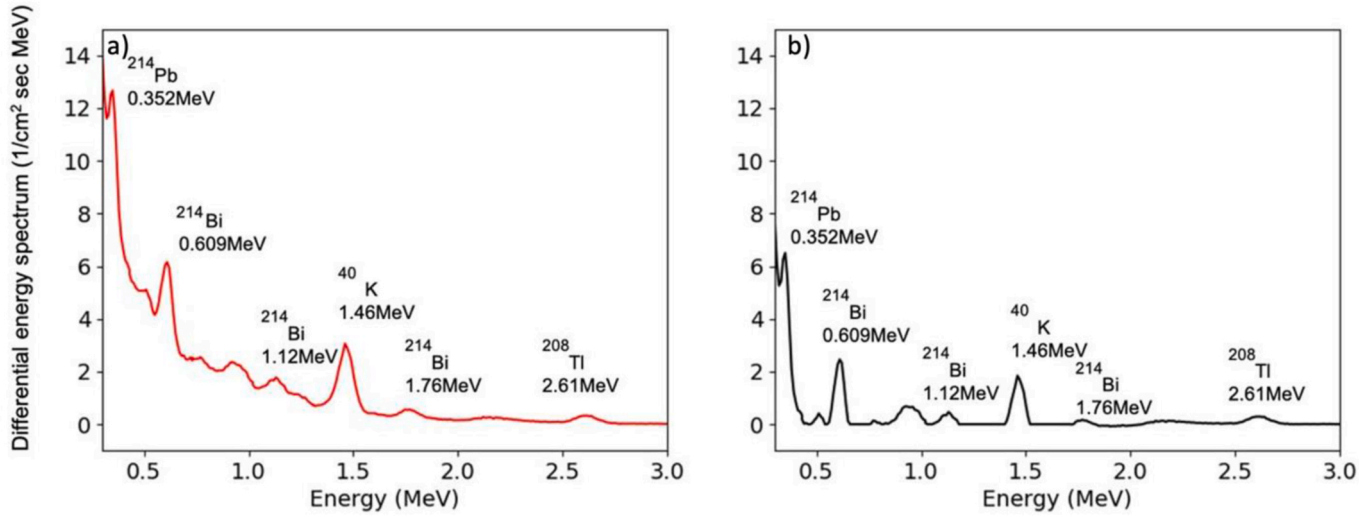

Fig. 5. NGR differential energy spectrum measured by ORTEC spectrometer before (a) and after (b) subtracting the CR contamination.

the low energy spectrum by subtracting the measurements of NaI N4 (with lead filter above) from NaI N2 (without lead filter). Then, after proper calibration, we subtract the obtained CR spectrum from the ORTEC spectrum (Fig. 5a) and readily obtain the "pure" NGR spectrum (Fig. 5b).

5. Huge enhancement of the ionizing radiation on May 23, 2023

On May 23, 2023, ASEC spectrometers detected a very large TGE. ORTEC spectrometer operated with a lead filter covering four sides and the bottom, with an open view above, see Fig. 2b. The NGR coming from the bottom and under large zenith angles was suppressed more than ten times. The goal of this arrangement was to suppress NGR to reveal CR enhancements maximally. As usual, we present the TGE flux by subtracting the fair-weather flux from the TGE maximum minute. As shown in Fig. 6, the CR particle flux (red curve) surpasses the background (blue curve) nearly eight times at low energies. The bump at ≈520 keV is due to positron annihilation producing 511 keV gamma rays coming from the near-vertical direction and cannot be filtered by lead. Thus, large TGE significantly contributes to NGR, enhancing gamma-ray radiation many times at energies of 300 keV–1 MeV.

6. The radon progeny gamma radiation in positive and negative NSEF

222Radon undergoes a decay sequence starting with alpha decay to form 218Polonium, which subsequently decays via another alpha emission to 214Lead. 214Lead then undergoes beta decay to become 214Bismuth. These alpha emissions ionize the surrounding air, creating ions that readily attach to nearby aerosol particles. This attachment facilitates the transport of radon progeny to aerosols through mechanisms such as condensation, where radon progeny condenses onto existing aerosol particles, and coagulation, where smaller aerosols collide and amalgamate, trapping the radon progeny within. These processes contribute to the vertical transport of radon progeny into the atmosphere.

To investigate the effects of NSEF on radon progeny detection, we analyzed four storm events characterized by positive (indicating downward-accelerated positrons) and negative (indicating downward-accelerated electrons) NSEF values. The observed NSEF values, measured in (kV/m), were as follows: positive fields at (5.6, 13.8, 9.8, 17.5) and negative fields at (−16.0, −14.8, −8.4, −6.0). Event on September 26, 2023, demonstrated a significant correlation between NSEF disturbances and radon progeny count rate (Fig. 7). The NSEF

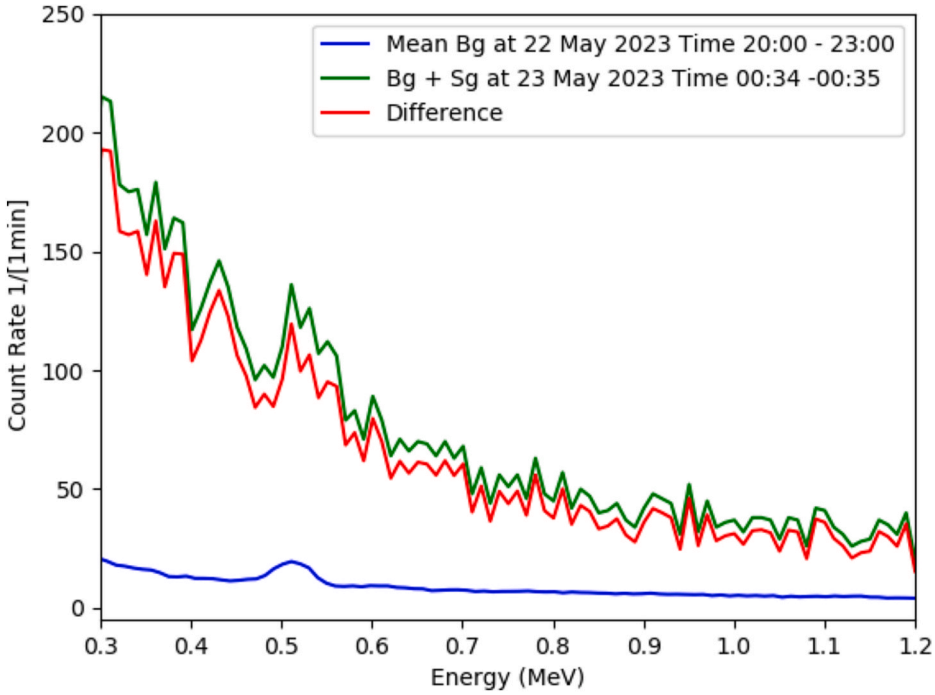

Fig. 6. The energy release histogram measured by ORTEC spectrometer at maximum TGE minute (green) and fair weather (blue). The residual red curve (green minus blue) represents the TGE energy release spectrum. The area of the ORTEC spectrometer is 0.0056 m^2. (For interpretation of the references to colour in this figure legend, the reader is referred to the Web version of this article.)

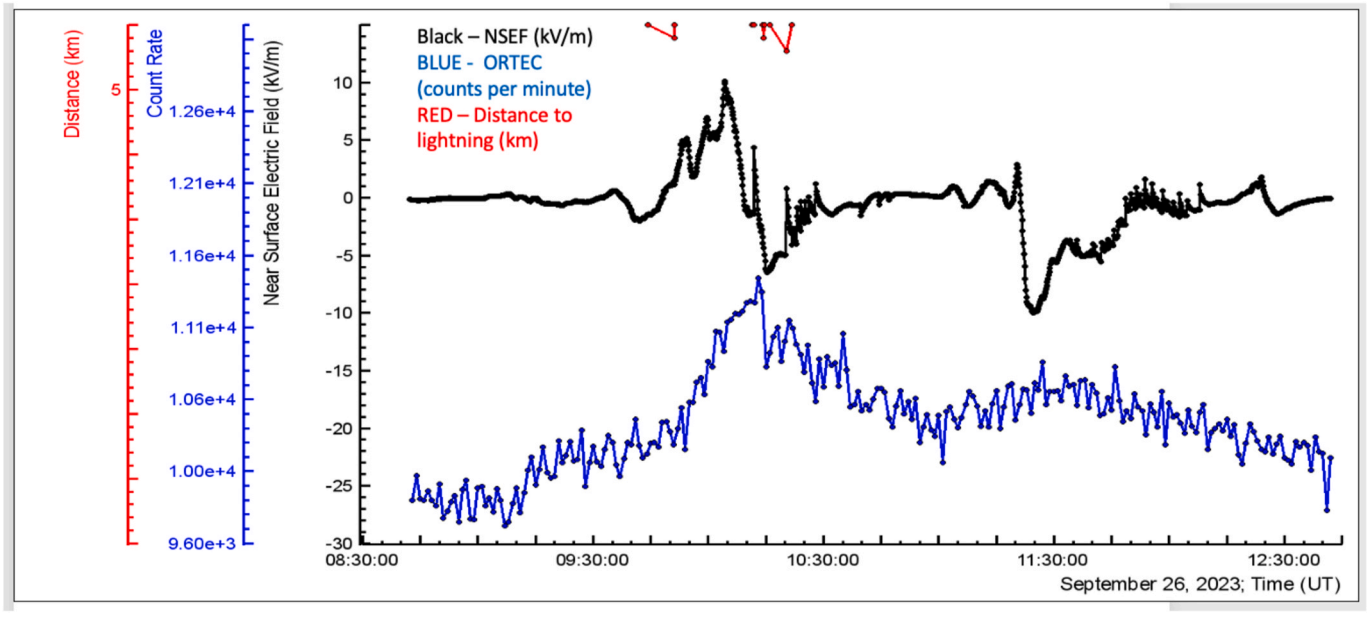

Fig. 7. NGR enhancement measured by ORTEC spectrometer at positive and negative NSEF measured by BOLTEK's EFM 100 electric mill.

peaked at five kV/m at 10:05, coinciding with a 15% increase in ORTEC's count rate from the baseline of approximately 10,000 to 11,500. Subsequently, as the radon progeny decayed, the count rate decreased until a surge associated with a negative NSEF occurred. 11:25 the NSEF reached −10 kV/m, while the ORTEC count increased to 10,900, exceeding the fair-weather baseline by 9%.

Table 2 presents the average intensities of NGR during fair weather (NGR0) and under positive (NGR+) and negative (NGR-) NSEF. The first row specifies the energies of isotopes' gamma emissions and the electron-positron annihilation peak at 511 keV. Due to the spectrometer's resolution limits, each isotope is attributed by falling in the energy ranges in the second row. Subsequent rows list the average intensities for several isotopes (in $cm^{-2}s^{-1}$) and the 511 keV line. The expected radiation doses at Aragats can be calculated from these intensities by simulating NGR flux interactions with the human body. The final row indicates the ratio of enhancements observed at positive and negative values of NSEF. Notably, due to positron acceleration, the 511 keV gamma-ray intensity is increased by a factor of 2.5 at positive NSEF. The radon progeny, with emission energies up to 1 MeV, shows an enhancement of 46–78% at positive NSEF compared to negative ones. In

Table 2
The summary table of NGR enhancement at positive and negative NSEF.

ORTEC Intensity 1/(cm^{2}sec)	Total intensity MeV	0.511 MeV	^{214}214Pb 0.352 MeV	^{214}Bi 0.609 MeV	^{214}Bi 0.768 MeV	0.84–3 MeV
Energy MeV	0.3–3	0.47–0.552	0.324–0.38	0.56–0.66	0.7–0.83	0.84–3
NGR^0	3,79 ± 0,07	0,09 ± 0,02	0,61 ± 0,3	0,79 ± 0,2	0,2 ± 0,04	2,1 ± 0,2
NGR^+	4,88 ± 0,4	0,19 ± 0,01	0,99 ± 0,2	1,08 ± 0,1	0,28 ± 0,01	2,35 ± 0,2
NGR^-	4,51 ± 0,6	0,13 ± 0,02	0,87 ± 0,3	0,97 ± 0,2	0,24 ± 0,05	2,3 ± 0,1
NGR^+-NGR^0	1,09	0,10	0,38	0,29	0,08	0,25
NGR^- -NGR^0	0,72	0,04	0,26	0,18	0,04	0,20
Ratio	1,5	2,5	1,5	1,6	2	1,25

contrast, the more abundant non-gaseous isotopes like 40K and 208 Tl, which have energies above 1 MeV, do not bind to aerosols, exhibiting minimal field-induced enhancements.

7. Conclusions

Our measurements have identified two significant additional sources of NGR: TGEs and radon progeny uplifted by NSEF during thunderstorms. We find that TGEs can increase NGR several times, while radon progeny contributes to a 20–30% enhancement. TGEs exhibit a brief duration of several minutes, whereas radon progeny radiation persists for 2–3 h.

An asymmetry was observed in the gamma radiation of radon progeny under positive and negative NSEF conditions. The positron flux, indicated by 511 keV annihilation gamma rays, was found to be 2.5 times higher during positive NSEF episodes. The same electric field, posited as a dipole between the lower positively charged region (Chilingarian et al., 2021) and its mirror, not only accelerates positrons towards the Earth but also causes the lifting of negatively charged aerosols. Given that NGR enhancement is 1.5–2 times more pronounced during positive NSEF (isotopes 214214 Pb and 214Bi), we infer a substantially higher concentration of negative aerosols near the Earth's surface during thunderstorms.

The global emergence of strong electric fields within the Earth's atmosphere during thunderstorms implies that the observed NGR enhancements are widespread phenomena. These effects warrant inclusion in the numerical models of Earth's atmospheric processes due to their significant planetary impact.

CRediT authorship contribution statement

A. Chilingarian: Conceptualization, Methodology, Project administration, Supervision, Visualization, Writing – original draft, Writing – review & editing. **B. Sargsyan:** Investigation, Methodology, Software, Validation, Visualization.

Declaration of competing interest

The authors declare that they have no known competing financial interests or personal relationships that could have appeared to influence the work reported in this paper.

Data availability

Data will be made available on request.

Acknowledgments

The data for this paper are available via the multivariate visualization software ADEI on the Cosmic Ray Division (CRD) web page of the Yerevan Physics Institute: http://adei.crd.yerphi.am/adei. We thank Gurgen Gabaryan, Karen Asatryan, and Edik Arshakyan for maintaining the Na (Tl) and ORTEC spectrometers, G. Hovsepyan for useful discussions, and V. Korogodina for the stimulating interest in measuring NGR on Aragats. The authors acknowledge the support of the Science Committee of the Republic of Armenia (Research Project No. 21AG-1C012) in the modernization of the technical infrastructure of high-altitude stations.

References

Abba, H.T., Saleh, M.A., Hassan, W.M.S.W., et al., 2017. Mapping of natural gamma radiation (NGR) dose rate distribution in tin mining areas of Jos Plateau, Nigeria. Environ. Earth Sci. 76, 208. https://doi.org/10.1007/s12665-017-6534-8.

Alexeenko, V.V., Khaerdinov, N.S., Lidvansky, A.S., et al., 2002. Transient variations of secondary cosmic rays due to the atmospheric electric field and evidence for pre-lightning particle acceleration. Phys. Lett. 301, 299–306.

Auger, P., Ehrenfest, P., Maze, R., et al., 1939. Extensive cosmic-ray showers. Rev. Mod. Phys. 11 (3–4), 288–291.

Babich, L.P., Kutsyk, I.M., Donskoy, E.N., et al., 2001. Comparison of relativistic runaway electron avalanche rates obtained from Monte Carlo simulations and kinetic equation solution. IEEE Trans. Plasma Sci. 29 (3), 430–438. https://doi.org/10.1109/27.928940.

Chilingarian, A., Arakelyan, K., Avakyan, K., et al., 2005. Correlated measurements of secondary cosmic ray fluxes by the Aragats Space-Environmental Center monitors. Nucl. Instrum. Methods Phys. Res., Sect. A 543 (2–3), 483–496.

Chilingarian, A., Daryan, A., Arakelyan, K., et al., 2010. Ground-based observations of Thunderstorm-correlated fluxes of high-energy electrons, gamma rays, and neutrons. Phys. Rev. D 82, 043009.

Chilingarian, A., Hovsepyan, G., Hovhannisyan, A., 2011. Particle bursts from thunderclouds: natural particle accelerators above our heads. Phys. Rev. D 83, 062001.

Chilingarian, A., Hovsepyan, G., Elbekian, A., Karapetyan, T., Kozliner, L., Martoian, H., Sargsyan, B., 2019. Origin of enhanced gamma radiation in thunderclouds. Phys. Rev. Res. 1, 033167.

Chilingarian, A., Hovsepyan, G., Sargsyan, B., 2020. Circulation of Radon progeny in the terrestrial atmosphere during thunderstorms. Geophys. Res. Lett. 47, e2020GL091155 https://doi.org/10.1029/2020GL091155.

Chilingarian, A., Hovsepyan, G., Svechnikova, E., Zazyan, M., 2021. Electrical structure of the thundercloud and operation of the electron accelerator inside it. Astropart. Phys. 132, 102615 https://doi.org/10.1016/j.astropartphys.2021.102615.

Chilingarian, A., Hovsepyan, G., Karapetyan, T., et al., 2022a. Measurements of energy spectra of relativistic electrons and gamma-rays avalanches developed in the thunderous atmosphere with Aragats Solar Neutron Telescope. J. Instrum. 17, P03002.

Chilingarian, A., Kozliner, L., Sargsyan, B., et al., 2022b. Thunderstorm ground enhancements: multivariate analysis of 12 years of observations. Phys. Rev. D 106, 082004.

Dwyer, J.R., 2003. A fundamental limit on electric fields in air. Geophys. Res. Lett. 30 (20), 2055. https://doi.org/10.1029/2003GL017781.

Gurevich, A.V., Milikh, G., Roussel-Dupre, R., 1992. Runaway electron mechanism of air breakdown and preconditioning during a thunderstorm. Phys. Lett. 165, 463.

Hossain, I., Sharip, N., Viswanathan, K.K., 2012. Efficiency and resolution of HPGe and NaI(Tl) detectors using gamma-ray spectroscopy. Sci. Res. Essays 7 (1), 86.

UNSCEAR, 1993. Sources, Effects, and Risks of Ionizing Radiation. UNSCEAR, United Nations, New York.

UNSCEAR, 2000. Sources and Effects of Ionizing Radiation. United Nations, New York.

Wada, Y., Matsumoto, T., Enoto, T., et al., 2021. Catalog of gamma-ray glow during four winter seasons in Japan. Phys. Rev. Res. 3, 043117.